Title

Coordination and Processing of DNA Ends During Double-Strand Break Repair: The Role of the Bacteriophage T4 Mre11/Rad50 (MR) Complex

Journal

Genetics, 195(3)

ISSN

0016-6731

Authors

Almond, Joshua R
Stohr, Bradley A
Panigrahi, Anil K
et al.

Publication Date

2013-11-01

DOI

10.1534/genetics.113.154872

Peer reviewed

Coordination and Processing of DNA Ends During Double-Strand Break Repair: The Role of the Bacteriophage T4 Mre11/Rad50 (MR) Complex

Joshua R. Almond,*,[1] Bradley A. Stohr,*,[1,2] Anil K. Panigrahi,*,[3] Dustin W. Albrecht,[†] Scott W. Nelson,[†] and Kenneth N. Kreuzer*,[4]

*Department of Biochemistry, Duke University Medical Center, Durham, North Carolina 27710, and [†]Department of Biochemistry, Biophysics and Molecular Biology, Iowa State University, Ames, Iowa 50011

ABSTRACT The *in vivo* functions of the bacteriophage T4 Mre11/Rad50 (MR) complex (gp46/47) in double-strand-end processing, double-strand break repair, and recombination-dependent replication were investigated. The complex is essential for T4 growth, but we wanted to investigate the *in vivo* function during productive infections. We therefore generated a suppressed triple amber mutant in the Rad50 subunit to substantially reduce the level of complex and thereby reduce phage growth. Growth-limiting amounts of the complex caused a concordant decrease in phage genomic recombination-dependent replication. However, the efficiencies of double-strand break repair and of plasmid-based recombination-dependent replication remained relatively normal. Genetic analyses of linked markers indicated that double-strand ends were less protected from nuclease erosion in the depleted infection and also that end coordination during repair was compromised. We discuss models for why phage genomic recombination-dependent replication is more dependent on Mre11/Rad50 levels when compared to plasmid recombination-dependent replication. We also tested the importance of the conserved histidine residue in nuclease motif I of the T4 Mre11 protein. Substitution with multiple different amino acids (including serine) failed to support phage growth, completely blocked plasmid recombination-dependent replication, and led to the stabilization of double-strand ends. We also constructed and expressed an Mre11 mutant protein with the conserved histidine changed to serine. The mutant protein was found to be completely defective for nuclease activities, but retained the ability to bind the Rad50 subunit and double-stranded DNA. These results indicate that the nuclease activity of Mre11 is critical for phage growth and recombination-dependent replication during T4 infections.

THE Mre11/Rad50 (MR) protein complex plays a central role in the response to double-strand breaks (DSBs) in eukaryotic cells (Stracker and Petrini 2011). The MR complex is quickly recruited to the site of DSBs, where its diverse functions include checkpoint activation mediated by the ataxia-telangiectasia mutated (ATM) kinase (Maser *et al.* 1997; Nelms *et al.* 1998; Lee and Paull 2005). Mutations in the human *Mre11* gene cause the ataxia-telangiectasia-like disorder, which is characterized by immunodeficiency, predisposition to certain cancers, and cellular hypersensitivity to ionizing radiation (Stewart *et al.* 1999).

The MR protein complex has been highly conserved throughout evolution, with homologs in *Saccharomyces cerevisiae*, *Pyrococcus furiosus*, *Escherichia coli* (SbcCD), and bacteriophage T4 (gp46/47) (Sharples and Leach 1995; Connelly and Leach 2002). The basic structure of the protein complex was elucidated in humans, *S. cerevisiae*, and *E. coli* (Connelly *et al.* 1998; Anderson *et al.* 2001; de Jager *et al.* 2001b; Hopfner *et al.* 2002). The core MR complex consists of an Mre11 dimer, with each Mre11 subunit bound to a single Rad50. Each Rad50 subunit adopts a long coiled-coil structure and can dimerize with a second Rad50 subunit through their so-called zinc hooks, a conserved Cys-X-X-Cys (CXXC, where X is any amino acid) motif at the apex of the coiled-coil domain that forms a zinc tetrathiolate center upon

doi: 10.1534/genetics.113.154872
Manuscript received June 28, 2013; accepted for publication August 16, 2013
[1]These authors contributed equally to this work.
[2]Present address: Department of Pathology, University of California, San Francisco, CA 94143.
[3]Present address: Department of Anesthesiology, Stanford University, Palo Alto, CA 94305.
[4]Corresponding author: Box 3711, Duke University Medical Center, Durham, NC 27710. E-mail: kenneth.kreuzer@duke.edu

dimerization. This Rad50 dimer serves as a flexible tether connecting Mre11 proteins on each end (Hopfner *et al.* 2002). The eukaryotic Mre11 protein has several conserved phosphoesterase motifs and in addition binds to double-stranded, single-stranded, and forked DNA structures (de Jager *et al.* 2001a; Connelly and Leach 2002; Trenz *et al.* 2006). The role of the Mre11 phosphoesterase activity in nucleolytic processing of the double-strand ends (DSEs) during repair was initially confusing, since the protein complex has an exonuclease activity with the wrong polarity for generating a 3′ resected end (Trujillo *et al.* 1998; Trujillo and Sung 2001; Lewis *et al.* 2004; Llorente and Symington 2004; Krogh *et al.* 2005). However, recent research has clarified a key role of the MR complex nuclease activity. MR (with partner proteins) removes a small segment of the 5′ terminal strand at a DSB and thereby licenses other exonucleases for efficient resection to generate the long 3′ single-stranded ends (Hopkins and Paull 2008; Mimitou and Symington 2008; Zhu *et al.* 2008).

The unique structure of the MR complex suggests that it could tether the ends of a DSB to facilitate proper repair (Cromie and Leach 2001; Connelly and Leach 2002; Williams *et al.* 2008). Indeed, the human MR complex can link two linear DNA strands *in vitro*, with the globular Mre11 proteins binding the DNA ends and the Rad50 zinc hooks interacting to tether the two DNA ends together (de Jager *et al.* 2001b). A similar role *in vivo* is supported by the work of Lobachev *et al.* (2004). While these results strongly argue that the MR complex plays a tethering role *in vivo*, the effect of tethering on DSB repair fidelity is not clear. Mutations in the MR complex can lead to genomic instability, but this instability could result from disruption of other MR complex functions such as checkpoint activation and telomere maintenance (Theunissen *et al.* 2003; Smith *et al.* 2005; Stracker and Petrini 2011).

Bacteriophage T4 provides a simple model system for DSB repair via homologous recombination, which has been studied using genetic, biochemical, and structural approaches. The phage encodes the UvsX strand exchange protein (Rad51 homolog), recombination mediator protein UvsY (Rad52 paralog), a branch-specific DNA helicase UvsW (most similar to eukaryotic Rad54), and the archetype single-strand binding protein gp32, all of which are involved in the strand exchange reaction (Yonesaki and Minagawa 1985; Formosa and Alberts 1986; Hinton and Nossal 1986; Kodadek *et al.* 1989; Yonesaki and Minagawa 1989; Morrical and Alberts 1990; Carles-Kinch *et al.* 1997; Gajewski *et al.* 2011). The mechanism of strand exchange between a single-stranded circle and homologous linear duplex has been studied in great detail *in vitro*, and crystallography has revealed three-dimensional structures of all or parts of the UvsX, UvsW, and gp32 proteins (Shamoo *et al.* 1995; Sickmier *et al.* 2004; Gajewski *et al.* 2011). Advantages of the T4 system include the limited number of involved proteins and the absence of complex post-translational modifications and other regulatory events in response to DNA damage, allowing a simpler view of the core recombination reaction.

Phage T4 also has a well-conserved homolog of the MR complex, which is necessary for DNA end processing *in vivo* but dispensable for strand exchange *in vitro* (in reactions that are initiated with a single-stranded substrate). The T4 MR complex consists of gp47 (the Mre11 homolog) and gp46 (the Rad50 homolog), which will hereafter be referred to as Mre11 and Rad50. The structure of the T4 MR complex has not been determined. However, the T4 homolog shows conservation of MR functional features, including the CXXC motif, Walker A and B motifs, signature motif, H- and D-loops, and heptad repeat region (presumed extended coiled coil) of the Rad50, along with the phosphoesterase motifs of Mre11 (Sharples and Leach 1995; Connelly and Leach 2002). Prior work in T4 has demonstrated that the MR complex is required for recombination-dependent replication (RDR) and DSB repair *in vivo* and is absolutely required for phage growth (reviewed in Kreuzer and Morrical 1994 and Kreuzer and Drake 1994). Interestingly, knockouts of the T4 MR complex are essentially lethal, while knockouts of other recombination proteins (UvsX, UvsY, UvsW) reduce the burst but are not lethal (Wiberg 1966; Cunningham and Berger 1977). This could reflect UvsXYW-independent recombination reactions (perhaps single-strand annealing) or could reflect some essential role for the MR complex outside of the RDR reaction (see *Discussion*). Consistent with results mentioned above with the eukaryotic protein, genetic studies support a role for the T4 MR complex in end coordination during DSB repair (Shcherbakov *et al.* 2006b; also see below).

Until very recently, the T4 MR complex was recalcitrant to purification and biochemical characterization. Limited success at purifying the complex was reported by Bleuit *et al.* (2001), but only small amounts of protein were obtained and the purification procedure was not reliable. However, Herdendorf *et al.* (2011) recently developed a robust procedure for purifying milligram amounts of the complex. The purified complex has activities very similar to the eukaryotic MR complex, including DNA-stimulated ATPase, 3′–5′ DNA (Mn^{++}-dependent) exonuclease, and single-stranded endonuclease activities (Herdendorf *et al.* 2011). This advance allowed characterization of the kinetics of ATP hydrolysis, modulation by partner proteins UvsY and gp32, and multiple biochemical analyses of substitution mutants in various functional motifs (Herdendorf *et al.* 2011; Herdendorf and Nelson 2011; De La Rosa and Nelson 2011; Albrecht *et al.* 2012). Perhaps most interesting is the finding that UvsY and gp32 activate a Mg^{++}-dependent endonuclease activity that was postulated to be involved in end resection (Herdendorf *et al.* 2011). One of the key questions that remain in the T4 system is whether the MR complex nuclease itself catalyzes extensive resection (in spite of the incorrect directionality of the exonuclease *in vitro*) or whether MR licenses another exonuclease(s), as in the eukaryotic system.

In this study, we have used the bacteriophage T4 model system to address *in vivo* roles of the MR complex. We find that reducing the amount of MR complex to growth-limiting (but not lethal) levels results in a profound defect in RDR of

the phage chromosome but only mild defects in DSB repair or in plasmid models of RDR. We also provide genetic evidence that these reduced levels of the MR complex result in more DNA end erosion and a strong deficiency in end coordination during DSB repair. Finally, we generated infections of phage with multiple different substitutions in the conserved histidine residue in phosphoesterase motif I of Mre11. Every tested substitution prevented phage growth and completely blocked RDR as measured by a DSB-dependent plasmid model system. We conclude that the Mre11 nuclease activity is critical for T4 growth and for RDR.

Materials and Methods

Materials

Restriction enzymes and T4 DNA ligase were purchased from New England Biolabs (Beverly, MA); 4–20% Mini-PROTEAN TGX gels and Precision Plus Dual Color Standards from Bio-Rad (Hercules, CA); O'GeneRuler DNA Ladder Mix from Thermo Fisher Scientific (Waltham, MA); goat anti-rabbit IR Dye 800CW from LI-COR Biosciences (Lincoln, NE); *E. coli* Proteins-Agarose affinity gel (for removing *E. coli* antibodies) from Alpha Diagnostic International (San Antonio, TX); Nytran Nylon Transfer Membrane from GE Healthcare (Waukesha, WI); Random Primed DNA Labeling Kit from Roche Diagnostics (Indianapolis); and [α-^{32}P] from PerkinElmer (Boston). Luria Broth (LB) was formulated as follows: Bacto-Tryptone (10 g/liter), yeast extract (5 g/liter), and NaCl (10 g/liter).

Strains

E. coli strains KL16-99 (CGSC #4206) (Hfr λ^- *e14*$^-$ *recA1 spoT1 thiE1 deoB13*) and CSH108 (CGSC #8081) [F′128 *Δ(gpt-lac)5* λ^- *ara(FG) gyrA-0(Nal*^{R}*) argE(Am) rpoB0(rif*^{R}*) thiE1*] were obtained from the Yale University *E. coli* Genetic Resource Center (New Haven, CT). The following *E. coli* strains were described previously: AB1 (nonsuppressing) (Kreuzer *et al.* 1988); MCS1 (*supD*) (Kreuzer *et al.* 1988); MV20 λ^+ (nonsuppressing, λ lysogen) (Stohr and Kreuzer 2002); MCS1 λ^+ (*supD*, λ lysogen) (Kreuzer *et al.* 1988); NapIV λ^+/pSTS54 (nonsuppressing, λ lysogen, RIIB expression plasmid) (Stohr and Kreuzer 2002); and CR63 (*supD*) (Edgar *et al.* 1964). The INTERCHANGE amber suppressor strains were purchased from Promega (Madison, WI). Suppressor-containing plasmids from the plasmid INTERCHANGE strains, along with plasmid pTD101, were moved into strain CSH108 for analysis of T4 RDR (Figure 6). The INTERCHANGE strains with chromosomal-borne suppressors are derivatives of CSH108.

Bacteriophage T4*td*SG2, which contains a deletion of the I-*Tev*I open reading frame (ORF), was generously provided by Marlene Belfort (State University of New York, Albany, NY) (Bell-Pedersen *et al.* 1990). T4 strain BAS3 is a derivative of T4tdSG2 with an I-*Tev*I ORF deletion and an I-*Tev*I recognition site interrupting the beginning of the *rIIB* gene (Stohr and Kreuzer 2002). The I-*Tev*I recognition site insert is 64 bp long, inserted between 168,894 and 168,895 bp of the T4 genome (T4 genome file NC_000866.4). T4 strain BAS4 is a double *rII* mutant, carrying the UV294 allele in *rIIA* (deletion of an extra T in run of T's at position 469–473 bp of the T4 genome) and the UV232 allele in *rIIB* (insertion of extra T in run of T's at position 168,468–168,469 bp). T4 strain FC11 harbors a frameshift mutation in *rIIB* resulting from deletion of one T in a run of T's at position 168,875–168,879 (Shinedling *et al.* 1987). T4 strains used for plasmid DNA replication experiments are derivatives of strain K10, which carries the following mutations: *am*B262 (gene *38*), *am*S29 (gene *51*), *nd*28 (*denA*), and *rIIPT8* (*denB-rII*$^\Delta$) (Selick *et al.* 1988).

The T4 derivatives with amber mutations at serine codons in gene *46*, including the triple amber mutant (*46*^{am3}), were constructed by performing marker rescue from pBR322-derived plasmids containing an internal fragment of gene *46* during an infection by T4tdSG2. The following serine residues were mutated in the indicated phage strains: Ser-303 (*46*^{am1} and *46*^{am3} mutants) and Ser-293 and Ser-296 (*46*^{am2} and *46*^{am3} mutants). The T4 K10 derivative with an amber mutation at the His-10 residue of gene *47* was constructed using the T4 insertion/substitution system (Selick *et al.* 1988). Additional T4 strains were constructed by genetic crosses.

Plasmids

Plasmids pBS4, pBS7, and pAC500 were described previously (Stohr and Kreuzer 2001; Stohr and Kreuzer 2002). Plasmid pBS4-0 is a derivative of pBS4 with the T4 replication origin removed (but it retains the I-*Tev*I recognition site; see diagram in Figure 4A). Plasmid pTD101 contains the I-*Tev*I recognition sequence, which suffers a DSB during bacteriophage T4 infection, flanked by direct repeats. It was derived from pTD001 (Tomso and Kreuzer 2000) as follows. Both plasmids pACYC184 and pTD001 were digested with *Ava*I and *Hin*dIII. The pACYC184 2848-bp fragment was ligated to the pTD001 2228-bp fragment to give pTD101.

Phage co-infections for growth and phage replication measurements

Phage co-infections were performed as described (Stohr and Kreuzer 2002). In brief, bacteria were grown to an OD_{560} of 0.5 and co-infected with the indicated phage strains at the indicated multiplicity of infection (MOI). After a 4-min adsorption at 37° without shaking, infections were continued with vigorous shaking. For determination of plaque-forming units (PFU) (Figure 1A), infected cells were lysed at indicated time points with chloroform at room temperature for 30 min, and cell debris was removed by centrifugation (8000 × *g* for 10 min). Lysate dilutions were then plated on *E. coli* CR63 to measure plaque formation. For determination of phage DNA replication during co-infection (Figure 1D), DNA was isolated from cell aliquots taken at the indicated time points as described previously (Stohr and Kreuzer 2001). Aliquots of isolated DNA were digested with PacI, a restriction enzyme that cuts modified T4 DNA, and

then subjected to Southern blotting using a probe consisting of the *Hin*dIII fragment with the *rIIA-rIIB* junction, labeled using the random primed method. Blots were visualized using a Phosphorimager and quantitated using ImageQuant software (Molecular Dynamics, Sunnyvale, CA).

Co-conversion and end coordination analysis

Co-infections were initiated as described above, and co-conversion and end coordination experiments were performed as described previously (Stohr and Kreuzer 2002). In brief, infected cells were lysed with chloroform after a 45-min infection, and cellular debris was removed by centrifugation. For co-conversion experiments, total phage titers and rII^+ recombinant phage titers were determined by plating lysate dilutions on MCS1 (λ^-) and MV20 λ^+, respectively. For end coordination experiments, phage titers were determined by plating on MV20 λ^+ (supports growth of rII^+ recombinants), MCS1 λ^+ (supports growth of $rIIA^-$ single mutants and rII^+ recombinants), and NapIV λ^+/pSTS54 (supports growth of $rIIB^-$ single mutants and rII^+ recombinants). Due to the low efficiency of plating on the NapIV λ^+/pSTS54 cell line, phage were preadsorbed to CR63 for 4 min before plating, as described previously (Stohr and Kreuzer 2002). All co-conversion and end coordination analyses were performed as previously described (Stohr and Kreuzer 2002).

Analysis of plasmid DSB formation and processing in T4-infected cells

The indicated bacterial strains were pregrown in LB containing appropriate antibiotic(s) with shaking at 37° to an OD_{560} of 0.5, and the indicated phage strain was then added at an MOI of 3. The infected cultures were incubated at 37° for 4 min without shaking to allow phage adsorption and then for 40 min with vigorous shaking. Aliquots were taken at 20 and 40 min, and total cellular DNA was purified using SDS/proteinase K treatment, phenol extraction, and dialysis as described previously (Stohr and Kreuzer 2001). The purified DNA was digested with the indicated restriction enzymes and subjected to agarose gel electrophoresis and Southern blotting. The probe for experiments with pTD101 consisted of a 1184-bp fragment of pACYC184 that had been doubly digested with *Xmn*I and *Drd*I. The probe for visualization of pBS4-0, pBS7, and pAC500 was generated using the random primed labeling kit with a mix of plasmids pBS7 (also hybridizes with pBS4-0) and pAC1000 (closely related to pAC500) as template.

Analysis of Mre11 expression levels after infection with 47^{am} (His-10) mutant

The growth and infection steps described immediately above for analysis of plasmid DSB formation and processing were used to produce cells infected with the indicated T4 phage for 20 min. The infected cells were collected by centrifugation in a microfuge, and the pellets were resuspended by vortexing in 500 μl of a wash buffer (100 mM NaCl, 50 mM Tris–HCl, pH 8, 1 mM EDTA). The cells were recollected by centrifugation and the supernatant was removed. The pellets were resuspended by vortexing in 25 μl of H_2O and then 25 μl of 2× SDS loading buffer (2.7 M glycerol, 0.1 M Tris, pH 6.8, 2% SDS, 0.29 M 2-mercaptoethanol, bromophenol blue at 10 mg/liter) was added. Samples were boiled for 5 min and debris was removed by centrifugation in a microfuge for 10 min. Total protein concentrations across samples were roughly equalized by subjecting each sample to polyacrylamide gel electrophoresis in triplicate, followed by staining with Coomassie Blue and quantitation using an Odyssey Infrared Imager (LI-COR Biosciences) and Odyssey Infrared Imaging System Application Software (LI-COR Biosciences, Version 3.0). The average intensities (using multiple bands) were compared between samples, and then the volumes were adjusted for equal loading of total protein on the final gel (Western blot below).

The samples were analyzed by Western blotting using a gp46/47 rabbit primary antibody that had been twice purified by passage over a total *E. coli* protein affinity gel. Samples were run on 4–20% Mini-PROTEAN TGX gels and then transferred to a nitrocellulose membrane using an iBlot (Invitrogen). The membrane was blocked with 5% nonfat milk buffer for 1 hr at room temperature. Next, 0.1% Tween 20 and a 400-fold dilution of the primary antibody were added into the blocking buffer and incubated overnight at 4° with shaking. The following day, the membrane was rinsed once with TBS-T [0.14 M NaCl, 0.02 M Tris–HCl (pH 7.6), 0.1% Tween 20] followed by three 10-min washes with TBS-T at room temperature. The membrane was next incubated with goat anti-rabbit IR Dye 800CW secondary antibody (1:20,000) in 5% nonfat milk buffer for 1 hr at room temperature with shaking. The membrane was rinsed with TBS-T once, followed by three 10-min washes with TBS-T at room temperature. Western blots were scanned using an Odyssey Infrared Imager (LI-COR Biosciences) and analyzed with the Odyssey Infrared Imaging System Application Software (LI-COR Biosciences, Version 3.0).

In vitro characterization of the H10S Mre11 mutant protein

The H10S mutation was generated in the Mre11 expression vector pTYB1-gp47 (Herdendorf *et al.* 2011) using the Quickchange mutagenesis protocol (Stratagene). The sequence of the forward mutagenic primer was 5′-gaaaattt taaatttaggtgattgg**agt**ttaggcgttaaagctgatgatg-3′, where the mutant codon is shown in boldface type. The second mutagenic primer was the reverse complement of the forward. The expression, purification, and biochemical assays were performed essentially as described (Herdendorf *et al.* 2011).

Results

Limiting the amount of MR complex by suppressing multiple amber mutations

The T4 MR complex is essential for viability (for review, see Mosig 1994). To investigate the function of the complex during a viable infection, we wanted to engineer a phage

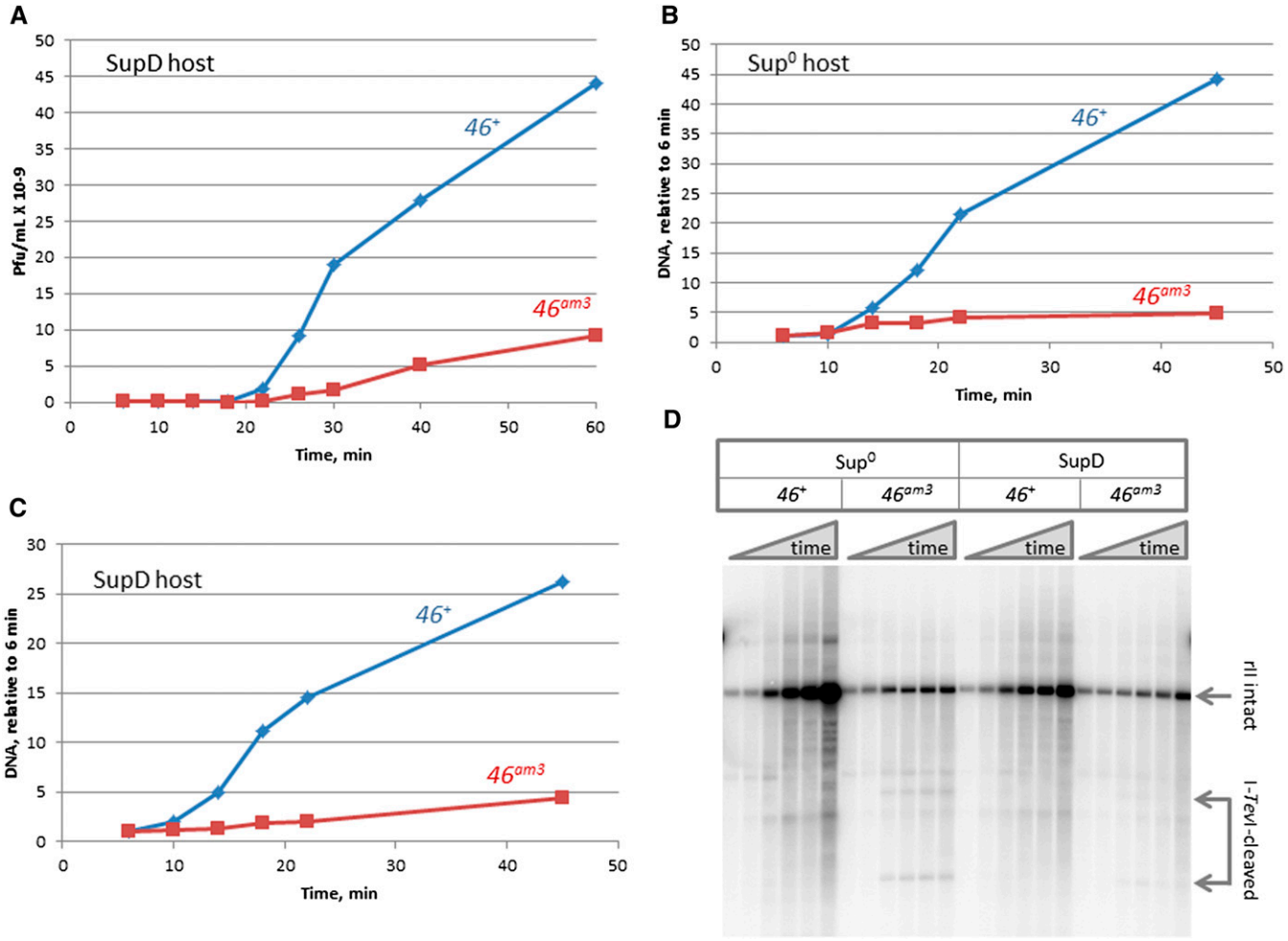

Figure 1 Limiting amounts of MR complex reduces phage burst size, DNA replication, and DSE processing. (A) Phage burst (PFU/ml) in the suppressor-containing *E. coli* strain CR63 after infection with T4 46^{+} (blue line) or T4 46^{am3} (red line). (B and C) Phage DNA amounts in nonsuppressing (B) and suppressing (C) *E. coli* strains after infection with T4 46^{+} (blue line) or T4 46^{am3} (red line) T4. DNA amounts were determined by quantitation of the intact *rII* bands on the Southern blot shown in D and are expressed relative to the levels at the first time point in each infection. (D) Intracellular DNA was isolated 6, 10, 14, 18, 22, and 45 min after infection of nonsuppressing (Sup^0; strain AB1) and suppressing (SupD; strain CR63) cells with 46^{+} or 46^{am3} phage. DNA was cleaved with *Pac*I restriction enzyme, and Southern blotting was performed using a probe for the *rII* region of the phage genome. Intact and I-*Tev*I-cleaved *rII* bands are indicated.

mutant with reduced and growth-limiting levels of MR complex. Such a mutant could potentially be used to demonstrate genetic defects due to limiting amounts of protein.

Many genetic studies of T4 utilize a serine suppressor (*supD*)-containing *E. coli* strain, CR63, to suppress amber mutations. This serine suppressor has been shown to function with efficiencies ranging from ~0.05 to just over 0.5 with various amber codons in different sequence contexts (Bossi 1983; Miller and Albertini 1983). To reduce the levels of the MR complex without changing the amino acid sequence, we changed serine codons in gene *46*, which encodes Rad50, into amber codons and suppressed them with the serine suppressor. The serine codons were all roughly in the middle of the gene-coding region (residues 293, 296, and 303, near the CXXC motif at residues 288–291). This region was chosen because a previously analyzed amber mutation in this region is lethal when not suppressed, demonstrating that the amber fragment does not substitute for the essential function(s) of the Rad50 subunit (data not shown).

We first generated a single and a double amber mutant. The double amber mutant should generate much less active Rad50 than the single (presumably the product of the efficiency of suppression at the two sites). The single amber mutant looked identical to a wild-type control when grown in the suppressing strain CR63, whereas the double amber mutant had a slightly reduced plaque size. However, in liquid infections, neither mutant showed a significant reduction in average burst size (data not shown). We therefore constructed a triple amber mutant to further reduce the amount of Rad50. In this case, plaque size was strongly reduced, and the average burst size went down to about a fifth of that of the wild type (Figure 1A; also see below). Infections by this triple amber mutant, called 46^{am3}, provide an opportunity to analyze the genetic effects of limiting MR complex in a T4 infection.

End processing and phage DNA replication during infections with limiting MR complex

Based on the phenotypes of gene *46* or *47* knockout mutants, the T4 MR complex is required for the processing of DSEs and also for the bulk of T4 DNA replication, which occurs by an RDR mechanism (for review, see Mosig 1994). We began by comparing DNA replication and end processing in an MR knockout infection *vs.* a limiting MR infection (*i.e.*, the 46^{am3} mutant in a nonsuppressing *vs.* serine-suppressing host). As will be explained in more detail below, these were actually co-infections with two different phage strains. In each case, cells were infected with a multiplicity of six phage that carry the normal I-*Tev*I-encoding gene but no inserted I-*Tev*I site, along with a multiplicity of one phage that has a deletion of the I-*Tev*I gene but has an I-*Tev*I site inserted in the *rIIB* gene. Both co-infecting phage are either wild type or triple amber for the *46* gene. In this way, the bulk replication results shown first can be compared directly with the genetic analyses of DSB repair below.

We isolated intracellular DNA at various times after infection, cleaved with a restriction enzyme that cuts modified T4 DNA (PacI), hybridized a Southern blot with an *rII* probe, and quantitated the total amount of phage genomic DNA (*rII* fragment) by Phosphorimager (image of blot is in Figure 1D and quantitation in Figure 1, B and C).

Beginning with the nonsuppressing host, the 46^{am3} mutant had the expected DNA arrest phenotype, with some DNA replication (presumably origin-dependent) early but very little additional replication as the infection progressed (Figure 1B). In addition, DNA broken at the I-*Tev*I site was clearly present beginning at the 14-min time point, and the broken ends were stabilized throughout the remainder of the infection (Figure 1D; I-*Tev*I-cleaved DNA was undetectable in the wild-type infection). These results are exactly as expected from previous studies of gene *46/47* knockout mutations (Albright and Geiduschek 1983; Kreuzer *et al.* 1995; Tomso and Kreuzer 2000).

Next, we consider the triple amber mutant infection of the suppressing host, in which the MR complex is limiting for growth. In this case, the amount of phage DNA replication was again dramatically reduced compared to the 46^{+} control, and the phage burst was substantially reduced compared to the wild type (DNA amounts in Figure 1C; phage production in Figure 1A). In addition, I-*Tev*I-cleaved ends could be detected in DNA from the triple-amber-mutant infection but not in DNA from the 46^{+} infection, beginning with the 14-min time point (Figure 1D). The intensity of the cleaved bands, however, was much weaker than in the nonsuppressing host, consistent with many of the DSBs undergoing a repair reaction when the T4 MR complex is present but limiting (also see below). We conclude that limiting amounts of MR complex causes a modest reduction in the processing efficiency of DSBs, as well as greatly reduced levels of phage DNA replication.

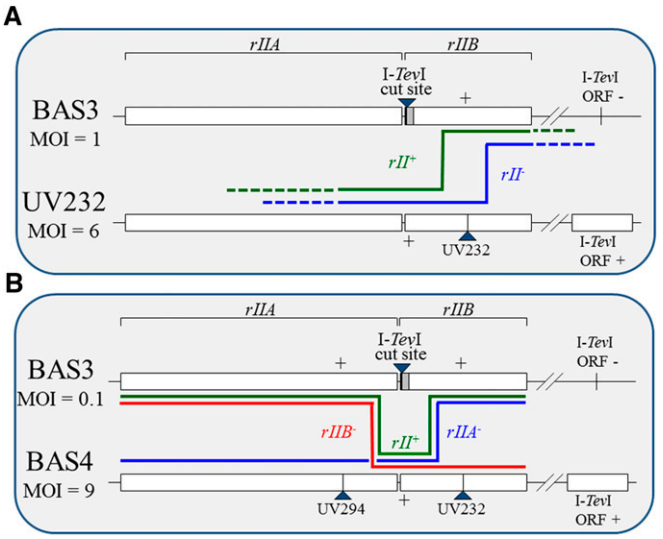

Figure 2 Diagram of recombination events during phage co-infections. (A) Co-conversion assay. Co-infections in strain CR63 (*supD*) are performed with one phage containing the I-*Tev*I cut site, while the other phage contains a single *rII* mutation (UV232 in the example shown). Depending on the processing of the DSB generated at the I-*Tev*I cut site, the resulting progeny molecules will be rII^{+} (green line) or rII^{-} (blue line). (B) End-coordination assay. Co-infections are performed with one phage containing the I-*Tev*I cut site and the other phage containing flanking UV294 and UV232 *rII* mutations. Generation of rII^{+} progeny (green line) will be higher if the two ends of the break are repaired in a coordinated fashion.

Recombination of linked markers during DSB repair with limiting MR complex

We next analyzed the effects of this reduction in MR complex levels on homologous recombination, using a genetic system for analyzing homologous recombination stimulated by defined DSBs within the *rIIB* gene (Stohr and Kreuzer 2002). This system monitors the contribution of nearby heteroalleles during the DSB repair reaction and can also be used to measure the coordination of DNA ends during repair.

We performed a series of genetic crosses, each involving two rII^{-} alleles (Figure 2A). One phage genome (BAS3 in Figure 2A) carried an insertion of a defined DSB site near the 5′ end of the *rIIB* gene. The insertion renders BAS3 phage $rIIB^{-}$ due to a frameshift, and the inserted site is cleaved efficiently by I-*Tev*I endonuclease when it is available during T4 infections. The second phage genome (lower DNA) carried a nearby *rII* heteroallele: FC11, UV232, or UV294, located 15, 425, or 460 bp (respectively) from the site of the I-*Tev*I site insertion. In each cross, both phage strains have either a wild-type gene *46* or the 46^{am3} allele. In addition, the BAS3 phage with the I-*Tev*I site insertion carries a deletion of the I-*Tev*I reading frame, and this protein is provided *in trans* by the phage that carries the FC11, UV232, or UV294 allele (see Figure 2A). The phage with a functional I-*Tev*I gene and the *rII* heteroallele is used at an MOI of 6, while the BAS3 phage is used at an MOI of 1. This ensures that nearly every BAS3 chromosome with an I-*Tev*I insertion site

Table 1 DSB-induced recombination analysis

Marker Distance (bp), direction from I-*Tev* I site	UV294 460, left	UV232 425, right	FC11 15, right
46^{+}, total PFU/mL	4.49 (± 0.41) × 10^{10}	4.05 (± 0.54) × 10^{10}	4.73 (± 0.32) × 10^{10}
46^{am3}, total PFU/mL	1.76 (± 0.54) × 10^{10}	1.45 (± 0.27) × 10^{10}	1.24 (± 0.04) × 10^{10}
46^{+}, *rII*$^{+}$/total PFU	0.062 ± 0.0060	0.069 ± 0.0035	0.0182 ± 0.0026
46^{am3}, *rII*$^{+}$/total PFU	0.045 ± 0.0106	0.049 ± 0.0040	0.0072 ± 0.00043
P-value, *rII*$^{+}$/total PFU	0.070	0.0029	0.0019
46^{+}, I-*Tev*I$^{\Delta}$/total PFU	0.152 ± 0.0089	0.157 ± 0.0116	0.147 ± 0.0207
46^{am3}, I-*Tev*I$^{\Delta}$/total PFU	0.137 ± 0.0118	0.127 ± 0.0171	0.120 ± 0.0001
46^{+}, co-conversion	0.590 ± 0.015	0.561 ± 0.025	0.876 ± 0.011
46^{am3}, co-conversion	0.675 ± 0.048	0.605 ± 0.067	0.940 ± 0.0035
P-value, co-conversion	0.0429	0.347	0.0007

This table summarizes data from triplicate infections according to the diagram in Figure 2A. Each data point presents the mean ± SD of the triplicate infections. *P*-values were calculated by a two-tailed unpaired *t*-test. Distance and direction from I-*Tev*I site is indicated, as drawn in Figure 2A. See text for further explanation and co-conversion frequency formula.

is cleaved successfully and that most DSB repair events use a chromosome without the I-*Tev*I insertion site as a repair template (see Stohr and Kreuzer 2002). In our previous study, we showed that the frequency of recombination events that generate *rII*$^{+}$ phage (using a heteroallele close to UV294) was reduced by ~4.5-fold when both infecting phage strains were deleted for the I-*Tev*I-coding sequence, demonstrating a strong dependence on DSB induction (Stohr and Kreuzer 2002).

When the DSB site in the BAS3 phage chromosome is repaired using the lower phage DNA as template, the site essentially undergoes a gene conversion event in which the insertion is converted to *rIIB*$^{+}$ sequence (see Stohr and Kreuzer 2002, for a discussion of our usage of the terms "gene conversion" and "co-conversion"). At some frequency, the flanking *rII* marker is co-converted with the DSB site, resulting in an *rII*$^{-}$ progeny molecule. An *rII*$^{+}$ progeny molecule is generated only when the flanking marker is *not* co-converted, as shown with the green line in Figure 2A.

A variety of interrelated genetic parameters were calculated from the results of these crosses (Table 1). First, we found that the frequency of *rII*$^{+}$ progeny phage was only modestly reduced in the MR-depleted infections with the heteroalleles UV294 and UV232 and was more substantially reduced with the very close FC11 marker (the UV294 difference was not quite statistically significant). As is described below, the more substantial reduction with FC11 may reflect the details of end processing locally at the break. Considering that a large majority of recombination events are dependent on DSB production (see above) and that MR depletion reduced the frequency of *rII*$^{+}$ progeny by only ~30% with the other two markers, we infer that DSB repair efficiency is not much affected by MR depletion.

Another measure of the frequency of DSB repair is provided by the survival of the DNA molecule that sustains the DSB. For this purpose, the distant I-*Tev*I gene deletion serves as an unlinked marker of the BAS3 chromosome. The calculated input fraction of the BAS3 chromosomes is 1/7 or 0.143 based on the MOIs. We measured the proportion of I-*Tev*I ORF deletion progeny phage from each infection by plaque hybridization to follow the possible loss of BAS3 chromosomes. As shown in Table 1, the output percentages were quite similar to the predicted input fraction for both the MR wild-type and MR-depleted infections. We measured ~15% (on average) fewer I-*Tev*I ORF deletion progeny phage from the MR-depleted infections, which rose to statistical significance ($P = 0.0014$) only when we combined the results from all nine infections (triplicates of the three heteroallele experiments). This small reduction is again consistent with a slightly lower frequency of DSB repair in the MR-depleted infection (although we cannot rule out the possibility that the small reduction results from some subtle technical problem). In any case, the most striking conclusion is that DSB repair again appears to be occurring at a near normal frequency in the MR-depleted infections.

As explained in more detail elsewhere, the co-conversion frequency of the linked heteroallele is calculated as 1 minus the ratio (*rII*$^{+}$ output percentage/I-*Tev*I ORF deletion output percentage) (see Stohr and Kreuzer 2002). In our previous study of *46*$^{+}$ infections, we found that the co-conversion frequency is very high near the break but drops off as a function of distance from the DSB (Stohr and Kreuzer 2002). We argued that exonuclease action starting at the break usually destroys the wild-type sequence on the cut chromosome when the flanking marker is very close to the break, but that the exonuclease action decreases stochastically with distance from the break (Stohr and Kreuzer 2002; also see Shcherbakov *et al.* 2006a).

For flanking markers that were 400–500 bp from the DSB site, such as UV232 and UV294, the co-conversion frequency in MR-proficient infections had dropped to ~0.5 (Stohr and Kreuzer 2002). If the MR complex is the major exonuclease involved in end processing, one might expect a substantial decrease in the co-conversion frequencies of markers like these in the MR-limiting infection due to reduced exonuclease action. However, we found that the frequencies of co-conversion for UV232 and UV294 were, if anything, slightly increased by the (suppressed) *46*^{am3} mutation (Table 1).

When we consider the same experiment with the FC11 marker, which is much closer to the DSB site (15 bp away), the results were more dramatic. Here, we found that the co-conversion frequency increased from 0.88 for the MR-proficient infection to 0.94 for the MR-limiting infection, a result that is extremely significant ($P = 0.0007$). Therefore, the reduced amount of Rad50 had a more significant effect on the behavior of a marker very close to a DSB site; the wild-type sequence in the cut chromosome (across from the FC11 allele) was apparently lost about twice as frequently in the MR-limiting infection than in the wild-type infection. This result is consistent with models in which the normal level of MR complex actually protects DNA from erosion very near the end (see *Discussion*).

Analysis of end coordination under conditions of limiting MR complex

The coordination of the two broken DNA ends during repair can be analyzed in a three-marker cross, with the DSB site between two flanking markers and the chromosome with the flanking markers being present in substantial excess (Figure 2B; note that in the subset of cells infected with BAS3 phage, a large majority will have a single infecting BAS3 phage chromosome with an average of nine infecting BAS4 chromosomes). The flanking markers in this experimental derivation are ones that give a frequency of co-conversion of ~0.5 (UV232 and UV294; see above). The basic rationale is that *rII*$^+$ recombinants are generated at a much higher frequency if the two broken ends are coordinated during the repair event, whereas uncoordinated repair (ends apart) would generate primarily *rII* single-mutant products from the DSB repair event (see Stohr and Kreuzer 2002). Thus, the ratio of *rII* single mutants to *rII*$^+$ phage recombinants reflects end coordination; a calculated ratio of ~16 reflects completely uncoordinated repair, while a ratio in the range of 1–4 reflects well-coordinated repair (the exact value depending on the repair model and assumptions within that model; see Stohr and Kreuzer 2002). We previously measured *rII* single mutant/*rII*$^+$ ratios of ~4.5 in MR-proficient infections, indicating that DSB repair in T4 generally does involve substantial end coordination (Stohr and Kreuzer 2002; also see Shcherbakov *et al.* 2006b).

We performed this same kind of experiment, directly comparing *46*$^+$ and *46*^{am3} infections (in the suppressing host). For technical reasons, we changed the *rIIA* marker from the one used in our previous analysis (HB80) to one that was at a similar location (UV294; these two are only 20 bp apart from each other). The ratio of *rIIB* single mutants to *rII*$^+$ recombinants was measured at 5.2 ± 0.43 for the *46*$^+$ infection (Table 2), close to the value measured by Stohr and Kreuzer (2002). However, this ratio increased very significantly to 8.2 ± 0.59 in the *46*^{am3} infection (Table 2; $P = 0.002$ for the difference, using two-tailed unpaired *t*-test). Therefore, depletion of the T4 MR complex leads to an apparent reduction in the coordination of DNA ends during repair of a DSB. A similar conclusion was reached using a distinct approach by Shcherbakov *et al.* (2006b).

Table 2 End coordination is reduced in MR-depleted infections

MR status	PFU/ml	*rII*$^+$/total PFU	*rIIB*$^-$/*rII*$^+$
Proficient (*46*$^+$)	4.18 (± 0.34) × 10^{10}	8.9 (± 1.1) × 10^{-4}	5.2 ± 0.43
Limiting (*46*^{am3})	0.88 (± 0.15) × 10^{10}	4.73 (± 1.0) × 10^{-4}	8.2 ± 0.59

This table summarizes data from triplicate infections according to the diagram in Figure 2B. Each data point presents the mean ± SD of the triplicate infections.

Also note that the frequency of *rII*$^+$ progeny in this three-factor cross was reduced about twofold in the MR-limiting infection (Table 2). The increased frequency of co-conversion of the two flanking markers in the MR-limiting infections should account for about half of this decrease, again consistent with the conclusion that DSB repair is only very modestly decreased in the MR-limiting infections.

Effects of MR depletion on plasmid-based model systems for DSB-induced RDR

Plasmid model systems provide useful windows for studying the details of phage T4 DSB processing/repair and the RDR that is induced during the DSB repair reactions (Kreuzer *et al.* 1995; George and Kreuzer 1996; Tomso and Kreuzer 2000; George *et al.* 2001; Stohr and Kreuzer 2002). These systems utilize phage derivatives carrying *denA* and *denB* mutations to prevent phage-induced plasmid DNA breakdown. Plasmid pTD101 carries a 787-bp duplication with an I-*Tev*I site located in between the direct repeats. This plasmid is very similar to the previously used plasmid pTD001, except that pTD101 is on a pACYC184 backbone while pTD001 is on a pBR322 backbone (see Tomso and Kreuzer 2000 for derivation of pTD001). After infection by T4, induction of I-*Tev*I leads to a DSB, and subsequent repair occurs predominantly by an RDR mechanism that generates rolling circle products with only one copy of the repeat per plasmid segment (Figure 3A) (Tomso and Kreuzer 2000; George *et al.* 2001).

As an independent means of analyzing the effect of MR depletion on T4 RDR reactions, we moved the *46*^{am3} mutation into a *denA denB* background and analyzed the phage-induced repair and replication of I-*Tev*I-cleaved pTD101. In a nonsuppressing host strain, infection with the *46*$^+$ control phage generated large amounts of replicated plasmid containing the expected deletion of one copy of the repeat ("replicated" band in Figure 3B). Restriction enzyme *Ase*I cuts T4-modified DNA and cleaves the plasmid once, allowing resolution of the unreplicated plasmid (full-length) and the replicated, deleted plasmid (replicated / A digests, Figure 3B). Addition of enzyme *Hae*III, which cuts unreplicated plasmid many times but is blocked by the T4 DNA modifications, demonstrates that only the replicated, deleted plasmid band carries the T4 DNA modifications diagnostic of T4-induced replication (A/H digests, Figure 3B). I-*Tev*I-cleaved DNA was processed efficiently in the *46*$^+$ infections and was thereby not detectable. When the *46*^{am3} mutant infected the nonsuppressing host, I-*Tev*I-cleaved DNA was greatly stabilized and T4-induced plasmid replication was completely

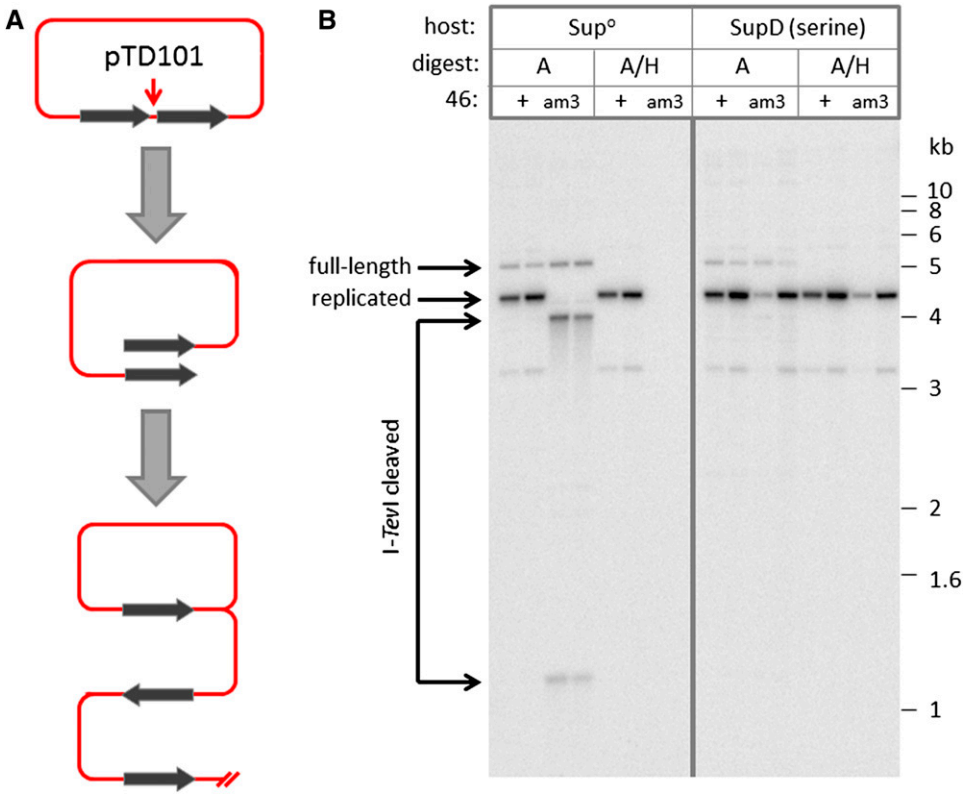

Figure 3 Impact of MR depletion on RDR of plasmid pTD101. (A) Diagram of plasmid pTD101, which contains direct repeats (thick black arrows) flanking an I-*Tev*I recognition site (red arrow). I-*Tev*I cleavage induces rolling circle replication as shown. (B) Southern blot showing pTD101 recombination and replication patterns following cleavage of the I-*Tev*I recognition site. Nonsuppressing (Sup^0; AB1) and suppressing (SupD; INTERCHANGE kit chromosomal strain with serine suppressor) hosts containing pTD101 were infected with *46*$^+$ or *46*^{am3} phage, and DNA was isolated at 20 and 40 min post-infection (left and right sample in each pair) and digested with *Ase*I alone (A) or with *Ase*I and *Hae*III (A/H). The band labeled "full length" represents an unreplicated plasmid containing both tandem repeats, while the band labeled "replicated" represents a phage-replicated plasmid containing only one of the two tandem repeats. The two shorter bands created by cleavage of the full-length plasmid band at the I-*Tev*I recognition site are indicated. The faint band migrating more slowly than the 3-kb marker (in this and some subsequent figures) is very likely due to star cutting of the replicated product by the restriction enzyme *Ase*I; relatively large amounts of *Ase*I are used in these reactions due to the difficulty of completely digesting the normal *Ase*I sites of T4-modified (hydroxymethylated and glucosylated) DNA.

blocked (am3, Figure 3B; note absence of DNA in the A/H digests). As expected, the *46*$^+$ infections of the *supD*-containing host looked identical to those in the nonsuppressing host, with abundant RDR plasmid product generation (Figure 3B). Finally, turning to the MR-depleted infections (*supD*/am3), we found that production of the plasmid RDR products was delayed but eventually reached levels that were nearly as high as in the *46*$^+$ infection (Figure 3B). Only a very small amount of I-*Tev*I-cleaved DNA was detected, indicating that end processing occurred in an efficient manner.

Phage genomic RDR appears to be much more severely inhibited by MR depletion than is RDR of the pTD101 plasmid model (compare results of Figure 1C and Figure 3B). We tested one possible explanation, namely that MR depletion preferentially inhibits intermolecular RDR (as in phage genomic) over intramolecular RDR (as in pTD101). For this purpose, we analyzed RDR in a two-plasmid system that allows both inter- and intramolecular RDR events from the same DSB (Stohr and Kreuzer 2002). I-*Tev*I-induced cleavage of plasmid pBS7 creates a broken plasmid that can undergo intramolecular RDR to generate a deleted product or intermolecular RDR when the broken end invades a partially homologous pAC500 plasmid (see diagram in Figure 4B). As a control, we also analyzed infections of cells containing pBS4-0 (no duplication) and pAC500, where only intermolecular RDR can occur. As expected, infection by the *46*$^+$ phage produced large amounts of replicated pAC500 (intermolecular) in both sets of infections and large amounts of replicated intramolecular product (pBS7 deletion) in only the pBS7/pAC500 infection (Figure 4C). In the MR-depleted infections (am3), a delayed but fairly robust production of plasmid RDR products was again observed, with no obvious discrepancy between intermolecular and intramolecular (Figure 4C). We conclude that MR depletion does not preferentially reduce either mode of RDR and that some other explanation is needed for the larger effect on phage genomic RDR (see *Discussion*).

Substitutions in the nuclease motif of the Mre11 subunit (gp47)

Studies in other systems have demonstrated the importance of the Mre11 phosphoesterase motifs, including the highly conserved motif I (Asp-X-His, where X is any amino acid) very near the N terminus (see Introduction). We are interested in the possible importance of the T4 Mre11 (gp47) nuclease activity, since the T4 MR complex is so important in DSE processing. To begin to test the importance of functional motifs and potentially uncover viable separation-of-function mutants, we mutated the highly conserved histidine (His-10) within motif I. Mutations in this motif of the *S. cerevisiae* Mre11 protein resulted in informative partial-function mutants (Krogh *et al.* 2005). Since any mutation of this highly conserved residue might turn out to be lethal in the T4 system, we introduced an amber mutation in place of the

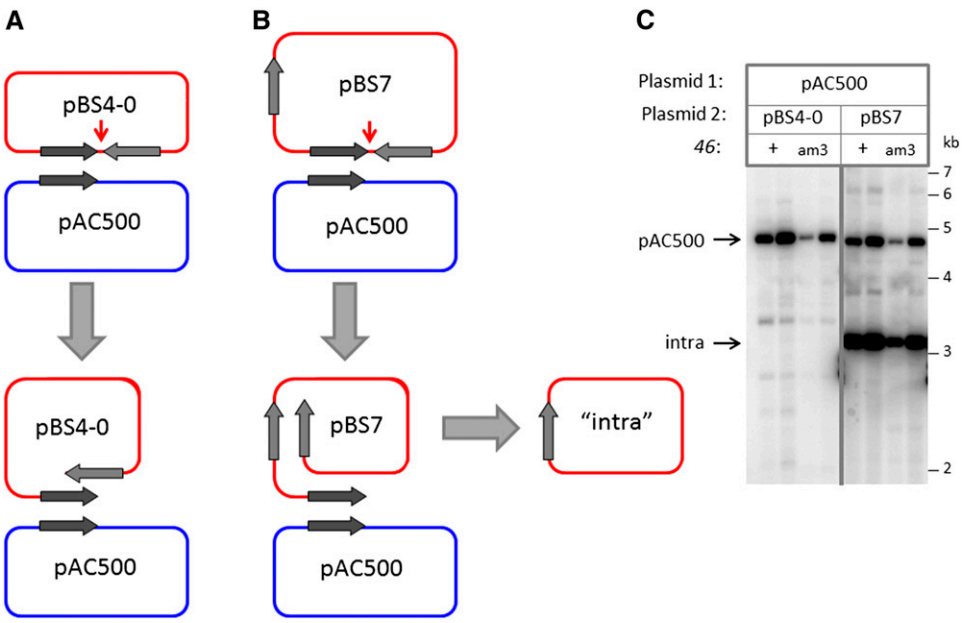

Figure 4 Impact of MR depletion on intermolecular and intramolecular plasmid RDR. (A and B) Diagrams of plasmid substrates. Thick dark gray and light gray arrows represent two different regions of homology shared between and/or within the plasmids. The I-*Tev*I cleavage site is indicated by the red arrow. In A, only intermolecular homologous recombination is possible due to the shared region of homology (dark-gray arrows). In B, both intermolecular and intramolecular homologous recombination occurs as diagrammed. (C) Southern blot showing patterns of plasmid RDR products. The serine-suppressing INTERCHANGE strain, containing plasmid pAC500 and either pBS4-0 or pBS7, was infected with 46^{+} or 46^{am3} phage. Strain K10 38^{+} 51^{+} and its 46^{am3} derivative were used for this experiment. DNA was isolated at 20 and 40 min post-infection (left and right sample in each pair) and digested with *Ase*I and *Hae*III. The phage-replicated bands resulting from intermolecular ("pAC500") and intramolecular ("intra") recombination are marked.

His codon and isolated the desired strain using a host containing a histidine-transfer RNA (tRNA) suppressor. The presence of the desired amber mutation ($47^{amHis10}$) in the resulting phage was confirmed by amplifying the region containing the mutation using the PCR and verifying the presence of an expected *Bfa*I restriction enzyme site.

We then took advantage of a collection of strains that each carry a different suppressor tRNA to introduce different amino acid substitutions at this residue (Kleina *et al.* 1990; Normanly *et al.* 1990), with the histidine-tRNA suppressor strain serving as positive control. The amber mutant phage failed to grow on multiple suppressor strains, implying that substitutions of lysine, arginine, proline, leucine, tyrosine, serine, glutamic acid, and glycine all result in lethality. Both the parental K10 strain and the $47^{amHis10}$ strain contain unrelated amber mutations in genes *38* and *51* (involved in tail and head assembly, respectively). Since the parental K10 strain grows in each of these suppressing hosts, the suppressor tRNAs must be functional (several other suppressing strains did not allow growth of either parental K10 or the $47^{amHis10}$ mutant, presumably due to lack of suppression of the *38* and/or *51* mutation). We conclude that the conserved histidine within phosphoesterase motif I of the T4 Mre11 is essential for T4 growth.

To test the importance of the histidine residue in motif I in T4 DSB processing and RDR, we used the plasmid RDR assay shown in Figure 3 above. Control infections with gene 47^{+} phage were conducted to test whether any of the suppressors interfere with T4 RDR for some trivial reason (*i.e.*, generating a dominant-negative replication protein due to readthrough).

Seven of the tested suppressors are plasmid-borne, and results with these strains are shown in Figure 5. The 47^{+} infection generated robust levels of plasmid pTD101 RDR product in the His, Cys, Pro, Glu, Arg, and Phe suppressor strains (with some delay in the Glu suppressor strain; Figure 5). However, infections of the Gly suppressor-containing strain consistently generated reduced levels of plasmid RDR product. The $47^{amHis10}$ phage, in contrast, generated plasmid RDR product only in the strain with the cognate His suppressor (Figure 5). Furthermore, the I-*Tev*I-cleaved plasmid bands were stabilized in each of the suppressor-containing strains (except His suppressor) after infection by the $47^{amHis10}$ phage. We conclude that DSE processing is inhibited and that RDR is completely blocked by these six substitutions at the His10 codon of the Mre11.

Five additional suppressors are located in the *E. coli* chromosome in a distinct genetic background. Since the efficiency of suppression can vary between genetic backgrounds, we introduced the His suppressor (on its pBR322-based plasmid) into the suppressor-free version of this genetic background as a positive control. The 47^{+} phage generated ample amounts of replicated pTD101 deletion product in either the suppressor-free or the His suppressor-containing host (Figure 6). Without any suppressor, the $47^{amHis10}$ phage generated no plasmid RDR product but robust amounts of stabilized I-*Tev*I-cleaved plasmid DNA, while the presence of the His suppressor effectively suppressed these defects (Figure 6). We conclude that this is a suitable genetic background to assess the effect of substitutions at the His-10 residue of the Mre11.

Turning to results with the five additional suppressors, the 47^{+} phage produced plasmid RDR product with little or

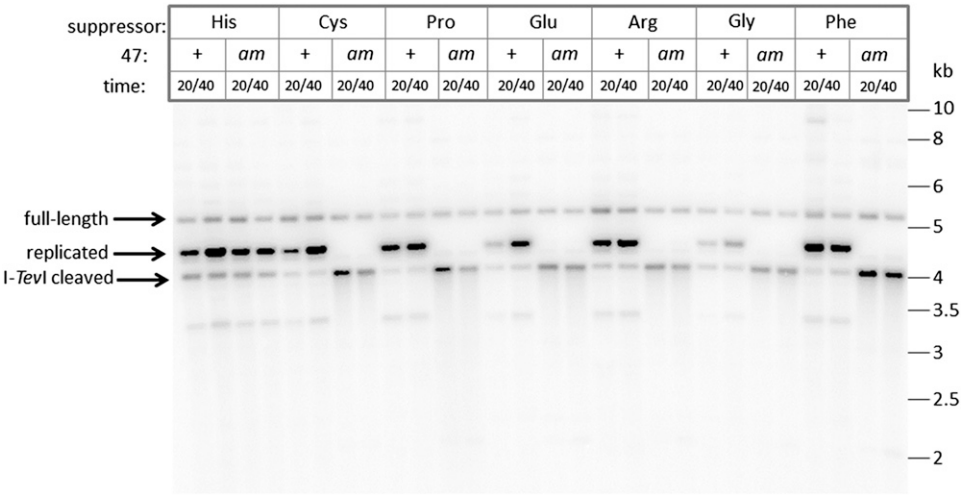

Figure 5 Plasmid RDR induced by T4 *47*^{amHis10} phage upon infection of cells with different plasmid-borne suppressors. *E. coli* KL16-99 cells that contained pTD101 and the indicated plasmid-borne suppressor were infected with either *47*$^{+}$ or *47*^{amHis10} phage, and samples were harvested after 20 and 40 min. Total DNA from the infections was digested with *Ase*I and analyzed by Southern blot with a pACYC184-derived probe. The *Ase*I digestion allowed for analysis of both phage-replicated and unreplicated (full-length and I-*Tev*I-cleaved) DNA.

no stabilization of the broken ends (Figure 7). Somewhat reduced levels of RDR product were seen in the Gln and Leu suppressor strains. In contrast, the *47*^{amHis10} phage produced no plasmid RDR product but did show robust amounts of stabilized I-*Tev*I-cleaved plasmid DNA in each of the strains (Figure 7).

We conclude that a wide range of substitutions at the His-10 codon of Mre11 abolishes the *in vivo* end processing and RDR activities of the T4 MR complex. These strong defects in end processing and RDR could be due to very poor suppression and/or production of unstable protein, which would trivialize the overall significance of these results. We therefore analyzed the level of soluble Mre11 in parallel infections by performing Western blots. Roughly equal amounts of total protein from 20-min infections of suppressor strains were compared. Considering the chromosomal suppressors, the tyrosine, serine, glutamine, and leucine suppressors all resulted in at least as much Mre11 as the positive control histidine suppressor, while the lysine suppressor resulted in very little protein (Figure 8). Considering the plasmid-based suppressors, the proline, glutamic acid, and glycine suppressors resulted in more Mre11 than the histidine suppressor, while the arginine, phenylalanine, and cysteine suppressors resulted in less (data not shown). Since the histidine suppressor appeared to be fully functional *in vivo* at its relative level of expression, we conclude that at least seven of the amino acid substitutions had sufficient levels of MR complex to sustain biological function but yet did not do so (while four others had lower levels of Mre11 that might have contributed to their lack of function). Therefore, at least seven substitutions of the His-10 codon block biological function even when expressed at levels sufficient for function with the wild-type Mre11, verifying the importance of the nuclease motif in Mre11 function.

Effect of the H10S mutation on the nuclease activity of Mre11

To confirm that mutation of the conserved motif I (Asp-X-His) of T4 Mre11 abolishes its nuclease activity, we generated the H10S (His-10 to Ser) point mutant in our pTYB1-gp47 expression plasmid, expressed the protein in *E. coli* BL21 (DE3) cells, and purified it to homogeneity. The mutant protein exhibited similar levels of expression and purified in an identical manner as the wild-type protein (data not shown). As predicted, the H10S mutant was completely defective in nuclease activity using two established nuclease assays. The first assay tests the ability of the MR complex to perform multiple nucleotide excisions on a uniformly ^{32}P-labeled, 1680-bp linear double-stranded DNA (dsDNA) and is dependent

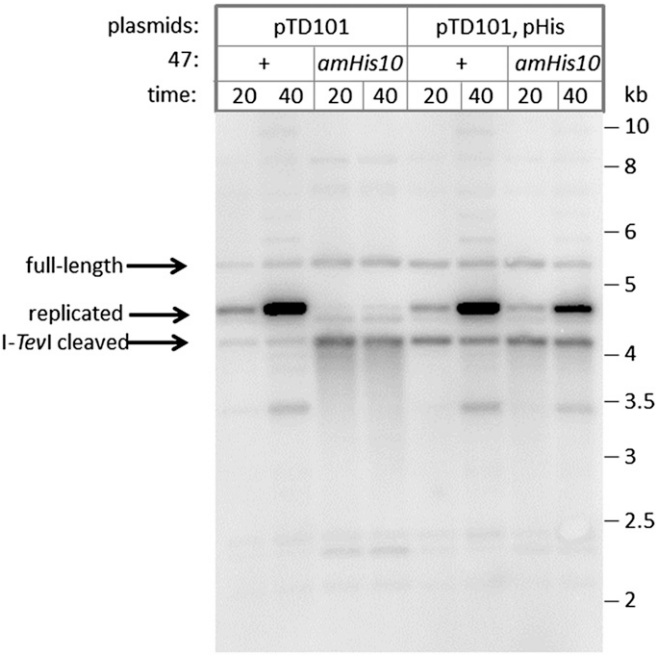

Figure 6 Plasmid RDR induced by T4 *47*^{amHis10} phage upon infection of cells with or without the plasmid-borne histidine suppressor. *E. coli* CSH108 cells that contained pTD101, with or without the plasmid-borne His suppressor, were infected with either *47*$^{+}$ or *47*^{amHis10} phage and samples were harvested after 20 or 40 min. Total DNA from the infections was digested with *Ase*I and analyzed by Southern blot with a pACYC184-derived probe.

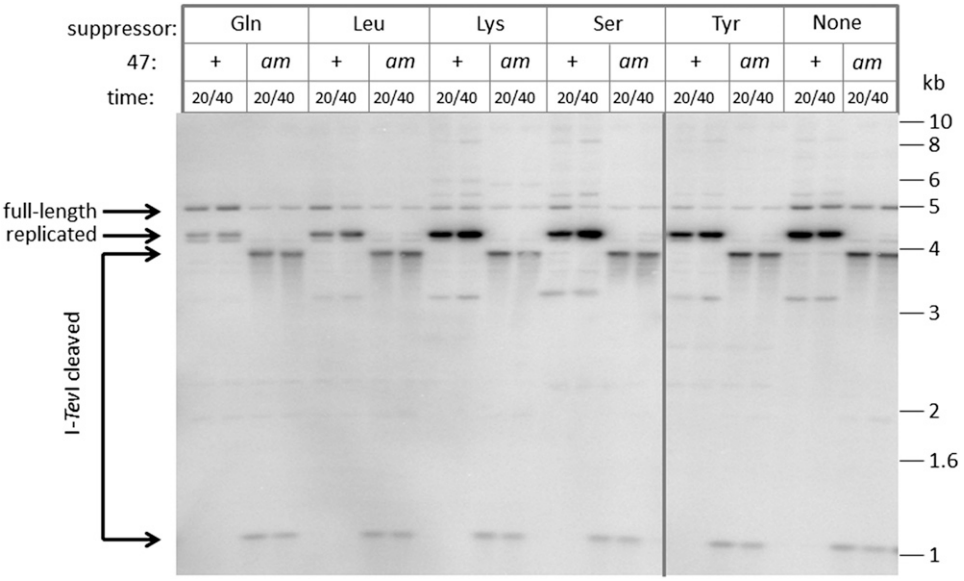

Figure 7 Plasmid RDR induced by T4 $47^{amHis10}$ phage upon infection of cells with different chromosome-borne suppressors. *E. coli* CSH108 cells that contained pTD101 and the indicated chromosomal-borne suppressor were infected with either 47^{+} or $47^{amHis10}$ phage, and samples were harvested after 20 or 40 min. Total DNA from the infections was digested with *Ase*I and analyzed by Southern blot with a pACYC184-derived probe.

on hydrolysis of ATP by Rad50 (Herdendorf *et al.* 2011). As shown in Figure 9A, the wild-type MR complex removes ~45% of the nucleotides during a rapid phase followed by a second, much slower phase. As described in Herdendorf *et al.* (2011), the data can be fit to a single-exponential plus linear equation, and control experiments have assigned these phases as dsDNA exo and single-stranded DNA exo/endo nuclease activities, respectively. The MR-H10S complex has no measurable activity during the time course of the reaction, consistent with the expected loss of nuclease activity due to the removal of this important metal ligating residue (Moreau *et al.* 1999; Hopfner *et al.* 2001). The second nuclease assay is performed under steady-state conditions and relies on the removal of the fluorescent nucleotide analog 2-aminopurine from the 3′ end of a 50-bp dsDNA substrate (Albrecht *et al.* 2012). In this assay, the Mre11 is activated by the presence of the Rad50, but ATP hydrolysis is not required. As seen in Figure 9B, the MR-H10S complex is also completely defective in ATP-independent nuclease activity.

To determine if H10S-Mre11 binds to both Rad50 and dsDNA, we performed ATP hydrolysis assays (Herdendorf *et al.* 2011). This assay is performed in the absence of $MnCl_2$ so that the nuclease activity of the wild-type Mre11 is absent. As shown in Figure 9C, the Rad50 alone has relatively little ATP hydrolysis activity, and the addition of either the Mre11 subunit or dsDNA alone has little effect. However, addition of either the wild-type or H10S-Mre11 together with DNA causes an ~20-fold activation in ATP hydrolysis activity of the Rad50. This indicates that the H10S-Mre11 retains its ability to bind to the Rad50 and that the H10S-MR complex binds to dsDNA in a normal fashion. Together, these results indicate that the H10S-Mre11 subunit is specifically defective in its nuclease activity but fully functional in complex assembly and DNA binding.

Discussion

The Mre11/Rad50 complex is a key factor in DSB repair and damage signaling that is conserved widely in evolution. We have investigated the detailed roles of the T4 MR complex by generating phage that produce growth-limiting amounts of the MR complex and also phage with substitutions in a conserved nuclease/phosphoesterase motif in Mre11.

Reducing the amount of T4 MR complex by suppression of three amber codons in the Rad50 gene with the cognate amino acid (*i.e.*, wild-type protein sequence) resulted in a substantial reduction in phage burst and dramatic reduction in phage RDR (Figure 1). The amount of phage DNA replication was not much higher than achieved with the complete knockout of MR protein upon infection of a suppressor-free host. We were able to investigate some of the details of MR function by use of this growth-limiting (but not lethal) situation.

A surprising aspect of the results is that the MR-depleted infection was nearly as defective in phage genomic RDR as the MR knockout infection, and yet the MR-depleted infection produced a modest burst while MR knockouts are essentially lethal. In a general sense, these results indicate that T4 requires some minimal level of MR complex to complete a growth-essential function. One model is that a very modest amount of MR-dependent RDR is necessary to generate concatameric DNA suitable for DNA packaging, and the MR-depleted infection can achieve this level of RDR. Another model involves the ends of the infecting T4 chromosome, which are bound by the end-protection protein gp2 (Silverstein and Goldberg 1976a,b; Oliver and Goldberg 1977; Lipinska *et al.* 1989). Eukaryotic MR complex is needed to liberate DNA from SPO11-DNA covalent complexes by means of an endonuclease reaction near the bound protein (for review, see Paull 2010). By analogy, perhaps the T4 MR complex is needed to generate free DNA ends in the infecting phage

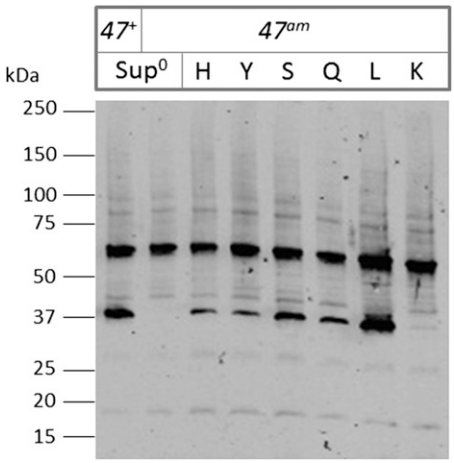

Figure 8 Western blot analysis of infections by T4 *47*^{amHis10} phage in cells with chromosomal-borne suppressors. *E. coli* CSH108 cells that contained pTD101 with no suppressor (first two lanes) or the plasmid-borne His suppressor (third lane) or chromosomal-borne suppressors (last five lanes) were infected with either *47*$^{+}$ (first lane) or *47*^{amHis10} (all other lanes) phage for 20 min. Roughly equal amounts of total protein from the infections were analyzed by Western blot with an MR complex (gp46/47) anti-rabbit primary antibody. Mre11 (gp47; 39.2 kDa) is the faster migrating band, while the slower migrating band present in every lane is an unidentified cross-reacting host protein (also present in uninfected cells). Rad50 (gp46) comigrates with the slower migrating band but has very poor reactivity with the antibody (data not shown).

DNA by cleavage near the bound gp2, with this reaction being debilitated in the MR-depleted infection but totally defective in the MR-knockout infection.

Another interesting, and perhaps related, issue is that the MR-depleted infections achieved relatively high levels of RDR when tested with the plasmid pTD101 system, in spite of the very low level of phage genomic RDR (Figure 3). One simple model was that MR depletion preferentially inhibits intermolecular over intramolecular RDR. We obtained evidence against this model by testing a two-plasmid system where both modes of RDR can occur (Figure 4). What then accounts for the different responses of plasmid *vs.* phage genomic RDR? Perhaps the above model for a role of MR complex in processing the natural, protein-bound genomic ends could explain the difference. The need for MR complex might be much higher with a protein-bound DSE than with the free DSEs generated after I-*Tev*I cleavage in the plasmid model systems. This would also be consistent with the relatively normal DSB repair when the phage genomic *rIIB* gene is cleaved with I-*Tev*I (Tables 1 and 2).

Despite the fact that MR-depleted infections showed reduced burst size and a strong reduction in phage genomic RDR, the efficiency and nature of DSB end processing and DSB repair seemed relatively normal. We detected very little accumulation of I-*Tev*I-broken DNA with either a phage genomic or a plasmid break (Figure 1D and Figure 3), which indicates that the broken ends were processed quickly and efficiently. Such broken ends are greatly stabilized in MR-knockout infections, indicating that the reduced amount of MR was important for the end processing. Also, the frequency of DSB repair as judged by genetic tests was only slightly reduced by the MR deficiency.

Genetic analysis using closely linked markers did reveal some interesting alterations in end processing of an inserted I-*Tev*I site in the MR-depleted infections (Table 1). We found a modestly reduced level of co-conversion of a linked marker ~425 bp from the insertion but a dramatic reduction in co-conversion for a marker only 15 bp from the insertion (Table 1). Some discussion of the molecular events underlying this genetic result is appropriate. Note first that the insertion consists of 64 bp of sequence with an I-*Tev*I cleavage site toward one end (Stohr and Kreuzer 2002). Therefore, the two 3′ ends of the broken DNA contain 53 and 13 extra bases that must be processed for correct DSB repair (I-*Tev*I cleavage is staggered by two bases with 3′ end overhangs; see Bell-Pedersen *et al.* 1991). Thus, the marker that is 15 bp from the insertion is actually 68 bp from the 3′ end of the broken DNA molecule. Regarding the resection events on the broken DNA, Shcherbakov *et al.* (2006a) showed that the T4 exonuclease DexA contributes to erosion of DNA only very near a break and that the T4 DNA polymerase proofreading exonuclease contributes to erosion of DNA both near and farther from a break (both tested in an MR-proficient infection). The simplest model to explain our results is that the reduced amount of MR complex in the suppressed triple amber mutant allows increased access to DexA exonuclease (given the strong effect that we see with the nearby marker FC11) and perhaps also to the T4 DNA polymerase exonuclease.

Using the MR-depleted infection, we have also asked whether the T4 MR complex helps to coordinate the repair of the two broken DNA ends. Results from a chromosomal DSB repair assay indicate that depletion of the T4 MR complex favors repair products in which the two ends of the break utilize different repair templates (Table 2). Using a distinct but related approach, Shcherbakov *et al.* (2006b) reached the same conclusion. They analyzed DSB repair in the very low numbers of progeny phage produced from MR-deficient infections and also in the higher numbers of progeny phage produced from MR-deficient phage that carry the *das* suppressor allele (which is believed to activate exonuclease activity of T4 RNase H; see personal communication in Shcherbakov *et al.* 2006b, pp. 782–783). These two studies together provide strong evidence that the MR complex prevents dissociation of the ends of a DSB, ultimately promoting a coordinated repair process. Perhaps the MR complex directly links the two ends together, as supported by *in vitro* activity of the MR complex (de Jager *et al.* 2001b). Alternatively, the MR complex might link the broken ends to the repair template, which would also keep the ends approximated (Hopfner *et al.* 2002).

Cromie and Leach (2001) proposed that, by linking the two ends of a DSB, the MR complex could limit the initiation of break-induced replication in favor of coordinated repair with only limited DNA synthesis at the break site. However, the repair products generated in our plasmid assays are fully

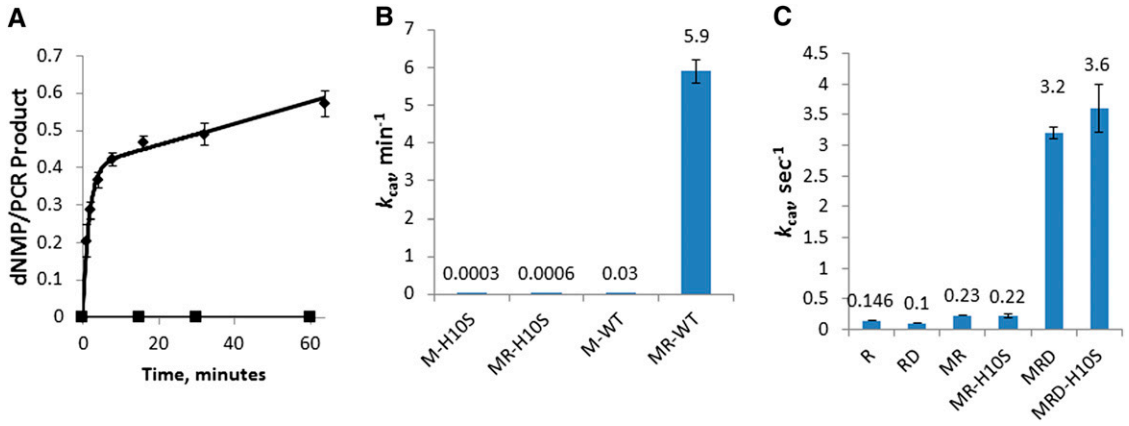

Figure 9 Biochemical characterization of the Mre11-H10S mutant. (A) Nuclease activity of the MR complex in the presence of ATP using a uniformly ^{32}P-labeled, 1680-bp dsDNA substrate. The wild-type and the H10S activity are represented by diamonds and squares, respectively. The solid lines are fits to the data as described in *Results*. (B) Steady-state exonuclease activity of the Mre11 subunit (M) and the MR complex (MR) for wild-type (WT) and the H10S mutant. The value shown above the bar represents the apparent k_{cat}. (C) Steady-state ATP hydrolysis activity of the Rad50 subunit (R) and the MR complex (MR). Assays performed in the presence of 50-bp linear dsDNA are indicated by the inclusion of the letter "D." In all cases, the data for the wild-type proteins come from Herdendorf *et al.* (2011).

replicated (also see George and Kreuzer 1996). Thus, our results imply that the MR complex can prevent the dissociation of the DNA ends even when the ultimate repair mechanism involves break-induced replication.

The need for coordinated repair of DSBs in eukaryotes is clear, as dissociation of the broken ends would lead to genomic instability. The role for coordination in T4 is less clear given the T4 life cycle. The extensive RDR during T4 infection leads to extensive recombination of the numerous genome copies, such that the entire replicating pool may comprise one large interconnected DNA mass (Mathews 1994). In this context, the value of tethering broken DNA ends in a T4 infection is uncertain.

We have also approached the biological role of the Mre11 nuclease active site. We found that at least eight different substitutions at the conserved His-10 residue abolish T4 growth, end processing, and RDR, demonstrating that this active site is critically important. Furthermore, we showed that a His10-to-Ser substitution abolishes the *in vitro* nuclease activity of the MR complex, while having no effect on DNA binding by the MR complex or stimulation of the Rad50 ATPase activity (Figure 9). These *in vitro* results can be directly compared with the complete defects in end processing and RDR *in vivo* when the $47^{amHis10}$ mutant infected a serine-suppressing host (Figure 7). The extreme phenotypes of the His10 substitutions in the Mre11 stand in contrast with the quite mild effects of substantial reductions in the MR complex in the suppressed triple amber (Rad50) infections.

As described above (see Introduction), the eukaryotic and *P. furiosis* MR complexes have 3′–5′ exonuclease activity as well as endonuclease activity, and the endonuclease activity on the 5′ strand is important for activating 5′–3′ exonucleases for strand resection. The activities of the T4 MR complex are very similar, although it is not yet clear whether it, too, activates other exonucleases for 5′–3′ resection (see Herdendorf *et al.* 2011). As described above, UvsY and gp32 activate a Mg^{++}-dependent endonuclease activity in the T4 MR protein that may be involved in end resection (Herdendorf *et al.* 2011). Our finding of a strict dependence of DSB end processing and repair on the Mre11 nuclease active site demonstrates the key nature of the nuclease activity of the T4 complex, but does not resolve the question of which enzyme catalyzes the extensive 5′-end resection in the DSB repair reaction.

While the role of the Mre11 nuclease motif in yeast and mammalian systems is complex and species-specific (Stracker and Petrini 2011), recent evidence in yeast and mammalian systems suggests that the nuclease motif of Mre11 is critical for many of its DNA repair functions. Mutations in the nuclease motif of the *Schizosaccharomyces pombe* Mre11 homolog caused hypersensitivity to DNA-damaging agents comparable to that of Mre11-deleted mutants (Williams *et al.* 2008). Similarly, mice either lacking Mre11 entirely or harboring a nuclease-deficient mutant Mre11 showed early embryonic lethality, and their cells were equally hypersensitive to ionizing radiation (Buis *et al.* 2008). Intriguingly, while the murine cells with nuclease-deficient Mre11 were defective in the activation of the ATR kinase, activation of the ATM kinase after DNA damage was not significantly impacted (Buis *et al.* 2008). Thus, the nuclease motif of Mre11 is critical for some but not all of its functions.

In summary, we have shown here that very low levels of wild-type MR complex results in relatively normal processing of induced DSBs in the phage T4 chromosome and relatively normal levels of plasmid RDR, but also leads to major deficiencies in both phage chromosomal RDR and end coordination. Further studies are needed to elucidate why these processes respond very differently to depleted MR levels and to test specific models involving processing the gp2 protein bound at genomic ends and/or a key role for

end coordination in phage chromosomal RDR. We also found that the nuclease motif in Mre11 is critically important for the plasmid model of RDR and for phage growth, with at least seven substitutions providing no complementing activity. One of these mutations was shown to directly abolish nuclease activity *in vitro* while preserving the ability of the mutant protein to interact with Rad50 and DNA. Future studies can now focus on the precise role of the nuclease motif either in activating nucleolytic processing by MR itself or by licensing some other nuclease for this key step in DSB repair.

Acknowledgments

We thank Melissa Kline for her technical contributions to this work. This work was supported by National Institutes of Health grant 5RO1 GM066934 (to K.N.K.) and National Science Foundation grant MCB:1121693 (to S.W.N.). J.R.A. was supported in part by grant T32CA009111 from the National Cancer Institute. The content of this article is solely the responsibility of the authors and does not necessarily represent the official views of the National Cancer Institute, the National Institute of General Medical Sciences, the National Institutes of Health, or the National Science Foundation.

Literature Cited

Albrecht, D. W., T. J. Herdendorf, and S. W. Nelson, 2012 Disruption of the bacteriophage T4 Mre11 dimer interface reveals a two-state mechanism for exonuclease activity. J. Biol. Chem. 287: 31371–31381.

Albright, L. M., and E. P. Geiduschek, 1983 Site-specific cleavage of bacteriophage T4 DNA associated with the absence of gene 46 product function. J. Virol. 47: 77–88.

Anderson, D. E., K. M. Trujillo, P. Sung, and H. P. Erickson, 2001 Structure of the Rad50 × Mre11 DNA repair complex from *Saccharomyces cerevisiae* by electron microscopy. J. Biol. Chem. 276: 37027–37033.

Bell-Pedersen, D., S. Quirk, J. Clyman, and M. Belfort, 1990 Intron mobility in phage T4 is dependent upon a distinctive class of endonucleases and independent of DNA sequences encoding the intron core: mechanistic and evolutionary implications. Nucleic Acids Res. 18: 3763–3770.

Bell-Pedersen, D., S. M. Quirk, M. Bryk, and M. Belfort, 1991 I-TevI, the endonuclease encoded by the mobile *td* intron, recognizes binding and cleavage domains on its DNA target. Proc. Natl. Acad. Sci. USA 88: 7719–7723.

Bleuit, J. S., H. Xu, Y. Ma, T. Wang, J. Liu *et al.*, 2001 Mediator proteins orchestrate enzyme-ssDNA assembly during T4 recombination-dependent DNA replication and repair. Proc. Natl. Acad. Sci. USA 98: 8298–8305.

Bossi, L., 1983 Context effects: translation of UAG codon by suppressor tRNA is affected by the sequence following UAG in the message. J. Mol. Biol. 164: 73–87.

Buis, J., Y. Wu, Y. Deng, J. Leddon, G. Westfield *et al.*, 2008 Mre11 nuclease activity has essential roles in DNA repair and genomic stability distinct from ATM activation. Cell 135: 85–96.

Carles-Kinch, K., J. W. George, and K. N. Kreuzer, 1997 Bacteriophage T4 UvsW protein is a helicase involved in recombination, repair and the regulation of DNA replication origins. EMBO J. 16: 4142–4151.

Connelly, J. C., and D. R. Leach, 2002 Tethering on the brink: the evolutionarily conserved Mre11-Rad50 complex. Trends Biochem. Sci. 27: 410–418.

Connelly, J. C., L. A. Kirkham, and D. R. Leach, 1998 The SbcCD nuclease of *Escherichia coli* is a structural maintenance of chromosomes (SMC) family protein that cleaves hairpin DNA. Proc. Natl. Acad. Sci. USA 95: 7969–7974.

Cromie, G. A., and D. R. Leach, 2001 Recombinational repair of chromosomal DNA double-strand breaks generated by a restriction endonuclease. Mol. Microbiol. 41: 873–883.

Cunningham, R. P., and H. Berger, 1977 Mutations affecting genetic recombination in bacteriophage T4D. I. Pathway analysis. Virology 80: 67–82.

de Jager, M., M. L. Dronkert, M. Modesti, C. E. Beerens, R. Kanaar *et al.*, 2001a DNA-binding and strand-annealing activities of human Mre11: implications for its roles in DNA double-strand break repair pathways. Nucleic Acids Res. 29: 1317–1325.

de Jager, M., J. Van Noort, D. C. Van Gent, C. Dekker, R. Kanaar *et al.*, 2001b Human Rad50/Mre11 is a flexible complex that can tether DNA ends. Mol. Cell 8: 1129–1135.

De la Rosa, M. B., and S. W. Nelson, 2011 An interaction between the Walker A and D-loop motifs is critical to ATP hydrolysis and cooperativity in bacteriophage T4 Rad50. J. Biol. Chem. 286: 26258–26266.

Edgar, R. S., G. H. Denhardt, and R. H. Epstein, 1964 A comparative genetic study of conditional lethal mutations of bacteriophage T4D. Genetics 49: 635–648.

Formosa, T., and B. M. Alberts, 1986 Purification and characterization of the T4 bacteriophage UvsX protein. J. Biol. Chem. 261: 6107–6118.

Gajewski, S., M. R. Webb, V. Galkin, E. H. Egelman, K. N. Kreuzer *et al.*, 2011 Crystal structure of the phage T4 recombinase UvsX and its functional interaction with the T4 SF2 helicase UvsW. J. Mol. Biol. 405: 65–76.

George, J. W., and K. N. Kreuzer, 1996 Repair of double-strand breaks in bacteriophage T4 by a mechanism that involves extensive DNA replication. Genetics 143: 1507–1520.

George, J. W., B. A. Stohr, D. J. Tomso, and K. N. Kreuzer, 2001 The tight linkage between DNA replication and double-strand break repair in bacteriophage T4. Proc. Natl. Acad. Sci. USA 98: 8290–8297.

Herdendorf, T. J., and S. W. Nelson, 2011 Functional evaluation of bacteriophage T4 Rad50 signature motif residues. Biochemistry 50: 6030–6040.

Herdendorf, T. J., D. W. Albrecht, S. J. Benkovic, and S. W. Nelson, 2011 Biochemical characterization of bacteriophage T4 Mre11-Rad50 complex. J. Biol. Chem. 286: 2382–2392.

Hinton, D. M., and N. G. Nossal, 1986 Cloning of the bacteriophage T4 UvsX gene and purification and characterization of the T4 UvsX recombination protein. J. Biol. Chem. 261: 5663–5673.

Hopfner, K. P., A. Karcher, L. Craig, T. T. Woo, J. P. Carney *et al.*, 2001 Structural biochemistry and interaction architecture of the DNA double-strand break repair Mre11 nuclease and Rad50-ATPase. Cell 105: 473–485.

Hopfner, K. P., L. Craig, G. Moncalian, R. A. Zinkel, T. Usui *et al.*, 2002 The Rad50 zinc-hook is a structure joining Mre11 complexes in DNA recombination and repair. Nature 418: 562–566.

Hopkins, B. B., and T. T. Paull, 2008 The *P. furiosus* Mre11/Rad50 complex promotes 5′ strand resection at a DNA double-strand break. Cell 135: 250–260.

Kleina, L. G., J. M. Masson, J. Normanly, J. Abelson, and J. H. Miller, 1990 Construction of *Escherichia coli* amber suppressor trna genes. II. Synthesis of additional tRNA genes and improvement of suppressor efficiency. J. Mol. Biol. 213: 705–717.

Kodadek, T., D. C. Gan, and K. Stemke-Hale, 1989 The phage T4 UvsY recombination protein stabilizes presynaptic filaments. J. Biol. Chem. 264: 16451–16457.

Kreuzer, K. N., and J. W. Drake, 1994 Repair of lethal DNA damage, pp. 89–97 in *Molecular Biology of Bacteriophage T4*, edited by J. D. Karam. American Society for Microbiology, Washington, DC.

Kreuzer, K. N., and S. W. Morrical, 1994 Initiation of DNA replication, pp. 28–42 in *Molecular Biology of Bacteriophage T4*, edited by J. D. Karam. American Society for Microbiology, Washington, DC.

Kreuzer, K. N., H. W. Engman, and W. Y. Yap, 1988 Tertiary initiation of replication in bacteriophage T4. Deletion of the overlapping *uvsY* promoter/replication origin from the phage genome. J. Biol. Chem. 263: 11348–11357.

Kreuzer, K. N., M. Saunders, L. J. Weislo, and H. W. Kreuzer, 1995 Recombination-dependent DNA replication stimulated by double-strand breaks in bacteriophage T4. J. Bacteriol. 177: 6844–6853.

Krogh, B. O., B. Llorente, A. Lam, and L. S. Symington, 2005 Mutations in Mre11 phosphoesterase motif I that impair *Saccharomyces cerevisiae* Mre11-Rad50-Xrs2 complex stability in addition to nuclease activity. Genetics 171: 1561–1570.

Lee, J. H., and T. T. Paull, 2005 ATM activation by DNA double-strand breaks through the Mre11-Rad50-Nbs1 complex. Science 308: 551–554.

Lewis, L. K., F. Storici, S. Van Komen, S. Calero, P. Sung *et al.*, 2004 Role of the nuclease activity of *Saccharomyces cerevisiae* Mre11 in repair of DNA double-strand breaks in mitotic cells. Genetics 166: 1701–1713.

Lipinska, B., A. S. Rao, B. M. Bolten, R. Balakrishnan, and E. B. Goldberg, 1989 Cloning and identification of bacteriophage T4 gene 2 product gp2 and action of gp2 on infecting DNA in vivo. J. Bacteriol. 171: 488–497.

Llorente, B., and L. S. Symington, 2004 The Mre11 nuclease is not required for 5′ to 3′ resection at multiple HO-induced double-strand breaks. Mol. Cell. Biol. 24: 9682–9694.

Lobachev, K., E. Vitriol, J. Stemple, M. A. Resnick, and K. Bloom, 2004 Chromosome fragmentation after induction of a double-strand break is an active process prevented by the RMX repair complex. Curr. Biol. 14: 2107–2112.

Maser, R. S., K. J. Monsen, B. E. Nelms, and J. H. Petrini, 1997 hMre11 and hRad50 nuclear foci are induced during the normal cellular response to DNA double-strand breaks. Mol. Cell. Biol. 17: 6087–6096.

Mathews, C. K., 1994 An overview of the T4 developmental program, pp. 1–8 in *Molecular Biology of Bacteriophage T4*, edited by J. D. Karam. American Society for Microbiology, Washington, DC.

Miller, J. H., and A. M. Albertini, 1983 Effects of surrounding sequence on the suppression of nonsense codons. J. Mol. Biol. 164: 59–71.

Mimitou, E. P., and L. S. Symington, 2008 Sae2, Exo1 and Sgs1 collaborate in DNA double-strand break processing. Nature 455: 770–774.

Moreau, S., J. R. Ferguson, and L. S. Symington, 1999 The nuclease activity of Mre11 is required for meiosis but not for mating type switching, end joining, or telomere maintenance. Mol. Cell. Biol. 19: 556–566.

Morrical, S. W., and B. M. Alberts, 1990 The UvsY protein of bacteriophage T4 modulates recombination-dependent DNA synthesis in vitro. J. Biol. Chem. 265: 15096–15103.

Mosig, G., 1994 Homologous recombination, pp. 54–82 in *Molecular Biology of Bacteriophage T4*, edited by J. D. Karam. American Society for Microbiology, Washington, DC.

Nelms, B. E., R. S. Maser, J. F. Mackay, M. G. Lagally, and J. H. Petrini, 1998 In situ visualization of DNA double-strand break repair in human fibroblasts. Science 280: 590–592.

Normanly, J., L. G. Kleina, J. M. Masson, J. Abelson, and J. H. Miller, 1990 Construction of *Escherichia coli* amber suppressor tRNA genes. III. Determination of tRNA specificity. J. Mol. Biol. 213: 719–726.

Oliver, D. B., and E. B. Goldberg, 1977 Protection of parental T4 DNA from a restriction exonuclease by the product of gene 2. J. Mol. Biol. 116: 877–881.

Paull, T. T., 2010 Making the best of the loose ends: Mre11/Rad50 complexes and Sae2 promote DNA double-strand break resection. DNA Repair (Amst.) 9: 1283–1291.

Selick, H. E., K. N. Kreuzer, and B. M. Alberts, 1988 The bacteriophage T4 insertion/substitution vector system. A method for introducing site-specific mutations into the virus chromosome. J. Biol. Chem. 263: 11336–11347.

Shamoo, Y., A. M. Friedman, M. R. Parsons, W. H. Konigsberg, and T. A. Steitz, 1995 Crystal structure of a replication fork single-stranded DNA binding protein (T4 gp32) complexed to DNA. Nature 376: 362–366.

Sharples, G. J., and D. R. Leach, 1995 Structural and functional similarities between the SbcCD proteins of *Escherichia coli* and the RAD50 and MRE11 (RAD32) recombination and repair proteins of yeast. Mol. Microbiol. 17: 1215–1217.

Shcherbakov, V. P., E. A. Kudryashova, T. S. Shcherbakova, S. T. Sizova, and L. A. Plugina, 2006a Double-strand break repair in bacteriophage T4: recombination effects of 3′-5′ exonuclease mutations. Genetics 174: 1729–1736.

Shcherbakov, V. P., L. Plugina, T. Shcherbakova, S. Sizova, and E. Kudryashova, 2006b Double-strand break repair in bacteriophage T4: coordination of DNA ends and effects of mutations in recombinational genes. DNA Repair (Amst.) 5: 773–787.

Shinedling, S., B. S. Singer, M. Gayle, D. Pribnow, E. Jarvis *et al.*, 1987 Sequences and studies of bacteriophage T4 rII mutants. J. Mol. Biol. 195: 471–480.

Sickmier, E. A., K. N. Kreuzer, and S. W. White, 2004 The crystal structure of the UvsW helicase from bacteriophage T4. Structure 12: 583–592.

Silverstein, J. L., and E. B. Goldberg, 1976a T4 DNA injection. I. Growth cycle of a gene 2 mutant. Virology 72: 195–211.

Silverstein, J. L., and E. B. Goldberg, 1976b T4 DNA injection. II. Protection of entering DNA from host exonuclease V. Virology 72: 212–223.

Smith, S., A. Gupta, R. D. Kolodner, and K. Myung, 2005 Suppression of gross chromosomal rearrangements by the multiple functions of the Mre11-Rad50-Xrs2 complex in *Saccharomyces cerevisiae*. DNA Repair (Amst.) 4: 606–617.

Stewart, G. S., R. S. Maser, T. Stankovic, D. A. Bressan, M. I. Kaplan *et al.*, 1999 The DNA double-strand break repair gene hMre11 is mutated in individuals with an ataxia-telangiectasia-like disorder. Cell 99: 577–587.

Stohr, B. A., and K. N. Kreuzer, 2001 Repair of topoisomerase-mediated DNA damage in bacteriophage T4. Genetics 158: 19–28.

Stohr, B. A., and K. N. Kreuzer, 2002 Coordination of DNA ends during double-strand-break repair in bacteriophage T4. Genetics 162: 1019–1030.

Stracker, T. H., and J. H. Petrini, 2011 The MRE11 complex: starting from the ends. Nat. Rev. Mol. Cell Biol. 12: 90–103.

Theunissen, J. W., M. I. Kaplan, P. A. Hunt, B. R. Williams, D. O. Ferguson *et al.*, 2003 Checkpoint failure and chromosomal instability without lymphomagenesis in Mre11(ATLD1/ATLD1) mice. Mol. Cell 12: 1511–1523.

Tomso, D. J., and K. N. Kreuzer, 2000 Double-strand break repair in tandem repeats during bacteriophage T4 infection. Genetics 155: 1493–1504.

Trenz, K., E. Smith, S. Smith, and V. Costanzo, 2006 ATM and ATR promote Mre11 dependent restart of collapsed replication forks and prevent accumulation of DNA breaks. EMBO J. 25: 1764–1774.

Trujillo, K. M., and P. Sung, 2001 DNA structure-specific nuclease activities in the *Saccharomyces cerevisiae* Rad50*Mre11 complex. J. Biol. Chem. 276: 35458–35464.

Trujillo, K. M., S. S. Yuan, E. Y. Lee, and P. Sung, 1998 Nuclease activities in a complex of human recombination and DNA repair factors Rad50, Mre11, and p95. J. Biol. Chem. 273: 21447–21450.

Wiberg, J. S., 1966 Mutants of bacteriophage T4 unable to cause breakdown of host DNA. Proc. Natl. Acad. Sci. USA 55: 614–621.

Williams, R. S., G. Moncalian, J. S. Williams, Y. Yamada, O. Limbo *et al.*, 2008 Mre11 dimers coordinate DNA end bridging and nuclease processing in double-strand-break repair. Cell 135: 97–109.

Yonesaki, T., and T. Minagawa, 1985 T4 phage gene UvsX product catalyzes homologous DNA pairing. EMBO J. 4: 3321–3327.

Yonesaki, T., and T. Minagawa, 1989 Synergistic action of three recombination gene products of bacteriophage T4, UvsX, UvsY, and gene 32 proteins. J. Biol. Chem. 264: 7814–7820.

Zhu, Z., W. H. Chung, E. Y. Shim, S. E. Lee, and G. Ira, 2008 Sgs1 helicase and two nucleases Dna2 and Exo1 resect DNA double-strand break ends. Cell 134: 981–994.

Communicating editor: S. Sandler